Journal of Zhejiang University SCIENCE
ISSN 1009-3095
http://www.zju.edu.cn/jzus
E-mail: jzus@zju.edu.cn

Three-dimensional nonlinear analysis of creep in concrete filled steel tube columns

CHENG Xiao-dong (程晓东)[†1,2], LI Guang-yu (李广宇)[2], YE Gui-ru (叶贵如)[†1]

([1]*Department of Civil Engineering, Zhejiang University, Hangzhou 310027, China*)

([2]*Hangzhou Municipal Infrastructure Development Corporation, Hangzhou 310006, China*)

[†]E-mail: cheng_xiaodong@163.com; ygr5812@mail.hz.zj.cn

Received Apr. 12, 2004; revision accepted July 6, 2004

Abstract: This paper proposes a based on 3D-VLE (three-dimensional nonlinear viscoelastic theory) three-parameters viscoelastic model for studying the time-dependent behaviour of concrete filled steel tube (CFT) columns. The method of 3D-VLE was developed to analyze the effects of concrete creep behavior on CFT structures. After the evaluation of the parameters in the proposed creep model, experimental measurements of two prestressed reinforced concrete beams were used to investigate the creep phenomenon of three CFT columns under long-term axial and eccentric load was investigated. The experimentally obtained time-dependent creep behaviour accorded well with the curves obtained from the proposed method. Many factors (such as ratio of long-term load to strength, slenderness ratio, steel ratio, and eccentricity ratio) were considered to obtain the regularity of influence of concrete creep on CFT structures. The analytical results can be consulted in the engineering practice and design.

Key words: Three-dimensional virtual laminated element (3D-VLE), Creep analysis, Three-dimensional viscoelastic theory, Three-parameters viscoelastic model, Concrete filled steel tube columns

doi:10.1631/jzus.2005.A0826 **Document code:** A **CLC number:** TU398

INTRODUCTION

Creep is an internal characteristic of concrete under long-term load. A long time has elapsed since the first discovery of concrete creep in 1907 by Hatt. Many researches have been devoted to this complex problem ever since. However, despite major successes, the creep phenomenon is still far from being fully understood, even though the phenomenon has occupied some of the best minds in the field, such as Glanville, Dischinger, Troxell, Pickett, Neville, etc. Creep phenomenon of CFT structures is relatively complex because core concrete is in multiaxial stress state. Past study often only considered the method of handling reinforced concrete in dealing with CFT structures and did not consider the interaction of steel tube and core concrete. So with more and more extensive applications of CFT in civil engineering, the effects of concrete creep should become more and more obvious.

Many experimental studies on creep in CFT columns had been conducted (Terry *et al*., 1994; Nakai *et al*., 1991; Tan and Qi, 1987; Qi, 1986; Ichinose *et al*., 2001). For theoretical calculation of the creep coefficient, there are mainly three kinds of methods extensively applied in actual engineering, which included schedule method, multi-ply coefficients method and composite function method. Summaries of experimental data include a series of theoretical formulas, the most representative formulas of which include CEB-FIP(1978) (CEIB, 1993), ACI(209) (ACI, 1992) and BP model. With the exception of BP model, all the other formulas involve a great deal of curves and tables, and some are inconvenient for use in numerical analysis. Bažant and Panula (1980) and Bažant (2001) presented two new prediction models for investigating concrete creep and shrinkage. One of them dealt with approximate prediction formulas for pore relative humidity distributions, required for realistic creep and shrinkage

analysis, and the other dealt with the extrapolation of short to long time measurements of creep and shrinkage. But the proposed method is only appropriate for pure concrete structures, and did not consider the interaction of steel tube and core concrete. A two parameters viscoelastic model was adopted to investigate the time-dependent behaviour of CFT columns and creep coefficients thus obtained were then compared with those recommended by the Japanese Specifications for Highway Bridges (Ichinose *et al*., 2001). The proposed model is directly applied to one-dimensional finite element analysis. So the simplified analysis may bring about many errors, as that core concrete is always in multiaxial stress state.

Based on above-mentioned findings, this paper proposes using the three-dimensional nonlinear viscoelastic theory to investigate the time-dependent behaviour of CFT columns. The method of 3D-VLE and a three parameters viscoelastic model, which represented the combined effect of the Maxwell and Voigt models, was developed to analyze the time-dependent effects. After the evaluation of the parameters of the proposed creep model, experimental measurements of two prestressed reinforced concrete beams can be applied for obtaining prediction curves accounting for the time-dependent behavior of the deformations and strains of CFT structures. Some CFT columns under long-term axial and eccentric load were analyzed by the proposed method. The experimental and calculated results accorded well. Many factors such as the ratio of long-term load to strength n, the slenderness ratio λ, the steel ratio ω, and the eccentricity ratio θ, were considered in this study on the regularity of the influence of concrete creep on CFT structures. The analytical results can be consulted in the engineering practice and design.

ANALYTICAL THEORY OF CONCRETE CREEP

Introduction of 3D-VLE

By the method of element blocking and laminated integral, a new-style element (3D-VLE) in which not only any element can be divided into many material blocks, but also different material blocks can be composed of different materials, even empty materials, was developed to study the mechanical behaviour of composite structures (Xu and Cai, 1993; Xu *et al*., 2002; Cheng *et al*., 2004a; 2004b). The merits of 3D-VLE are obvious. By introducing virtual nodes to describe the structure's geometry, deform performance, etc., and dividing elements into many blocks, the discretization of composite structures with varied cross section and depth can be easily dealt with. By this way, the number of needed elements can be greatly decreased, and computing procedure is simplified, while the required precision for engineering can be easily achieved. On the other hand, we can avoid dealing with the contact problems arising from the material diversities on the structural cross-section by dividing an element into many different material blocks.

Interpolation model of coordinates and displacement in 3D-VLE

The coordinates system of 3D-VLE is shown in Fig.1. Its interpolation models of coordinates and dis-

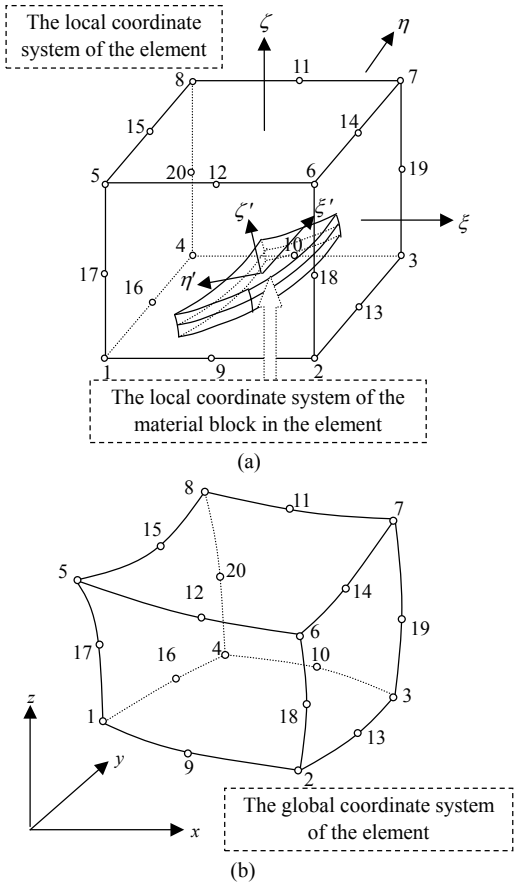

Fig.1 The coordinate system in 3D-VLE
(a) The local coordinate system; (b) The global coordinate system

placement are similar to those of three-dimensional isoparametric element's, and can be written as

$$\begin{Bmatrix} x \\ y \\ z \end{Bmatrix} = \sum_{i=1}^{20} N_i(\xi,\eta,\zeta) \begin{Bmatrix} x_i \\ y_i \\ z_i \end{Bmatrix}, \quad \begin{Bmatrix} u \\ v \\ w \end{Bmatrix} = \sum_{i=1}^{20} N_i(\xi,\eta,\zeta) \begin{Bmatrix} u_i \\ v_i \\ w_i \end{Bmatrix} \tag{1}$$

where $N_i(\xi,\eta,\zeta)$ is the same as the standard shape function of the three-dimensional 20-node isoparametric element.

Because the element may include different material blocks, the integral of the element stiffness and mass matrix will be dealt with according to the block. Generally, supposing that any material block can be determined by 8~20 points in the element (Fig.1), and that every point can be represented by its local coordinates in the element. We define these 8~20 points as the inner nodes of the element. If the local coordinate of the *i*th node in the *k*th material block can be marked as $(\xi_i^k,\ \eta_i^k,\ \zeta_i^k)$, then the local coordinate of any point in the *k*th material block can be written as

$$\begin{cases} \xi^k = \sum_{i=1}^{nm} N_i(\xi',\ \eta',\ \zeta')\xi_i^k \\ \eta^k = \sum_{i=1}^{nm} N_i(\xi',\ \eta',\ \zeta')\eta_i^k \\ \zeta^k = \sum_{i=1}^{nm} N_i(\xi',\ \eta',\ \zeta')\zeta_i^k \end{cases} \tag{2}$$

where $\xi'\in[-1,+1]$, $\eta'\in[-1,+1]$, $\zeta'\in[-1,+1]$, and *nm* is the number of the inner nodes representing the *k*th material block of element, $N_i(\xi',\ \eta',\ \zeta')$ is the same as the standard shape function of three-dimensional 20-node isoparametric element.

According to the standard process of the finite-element method, the element stiffness matrix of 3D-VLE can be derived by taking advantage of the virtual work principle. Its 3×3 submatrix $[k_{ij}]$ has the form of

$$[K_{ij}]_{3\times3} = \sum_{k=1}^{nb} \int_{-1}^{1}\int_{-1}^{1}\int_{-1}^{1} [\boldsymbol{B}_i(\xi^k,\eta^k,\zeta^k)]^{\mathrm{T}} \cdot [\boldsymbol{D}^k] \cdot \left[\boldsymbol{B}_j(\xi^k,\eta^k,\zeta^k)\right] |J||J'| \mathrm{d}\xi'\mathrm{d}\eta'\mathrm{d}\zeta' \tag{3}$$

where *nb* is the number of the material blocks in the *ie*th element, $[\boldsymbol{D}^k]$ is the elasticity matrix of the *k*th material block, $|J|$ and $|J'|$ are the Jacobian's valuation.

Three-parameters viscoelastic model

Creep phenomenon is an internal characteristic of concrete under long-term load. In this paper, a three-parameters viscoelastic model (Fig.2), which represents the combined effect of the Maxwell and Voigt models, is proposed for studying creep phenomenon of CFT structures. There is the following expression to describe the model

$$\begin{cases} \sigma = E_1\varepsilon_1,\ \sigma_1 = E_2\varepsilon_2,\ \sigma_2 = \eta\dot{\varepsilon}_2 \\ \sigma = \sigma_1 + \sigma_2,\ \varepsilon = \varepsilon_1 + \varepsilon_2 \end{cases} \tag{4}$$

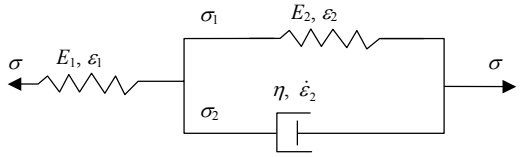

Fig.2 A three-parameters viscoelastic model

From Eq.(4), we can deduce the differential constitutive relationship as follows

$$\varepsilon + q_1\dot{\varepsilon} = p_0\sigma + p_1\dot{\sigma} \tag{5}$$

where: $q_1 = \dfrac{\eta}{E_2}$, $p_0 = \dfrac{E_1+E_2}{E_1E_2}$, $p_1 = \dfrac{\eta}{E_1E_2}$, and η is viscosity coefficient.

Increment viscoelastic constitutive relations

In 1876, Boltzmann proposed the Boltzmann's superposition principle, whose integral form can be written as

$$\varepsilon(t) = \sigma_0 J(t) + \int_0^t \frac{\mathrm{d}\sigma(\varsigma)}{\mathrm{d}\varsigma} J(t-\varsigma)\mathrm{d}\varsigma,$$

$$\text{or } \sigma(t) = \varepsilon_0 G(t) + \int_0^t \frac{\mathrm{d}\varepsilon(\varsigma)}{\mathrm{d}\varsigma} G(t-\varsigma)\mathrm{d}\varsigma \tag{6}$$

Eq.(6) is so-called generic integral and shows that the strains of viscoelastic materials are related to the loading history. We usually suppose that the load time begins at t=0 and ε_0=σ_0=0.

If we solve differential Eq.(5), the following expression will be easily obtained

$$\sigma(t)=g_0\varepsilon(t)+\int_0^t g_1\mathrm{e}^{-\alpha(t-\tau)}\frac{\mathrm{d}\varepsilon(\tau)}{\mathrm{d}\tau}\mathrm{d}\tau \tag{7}$$

where $\alpha=\dfrac{E_1+E_2}{\eta}$, $g_0=\dfrac{E_1E_2}{E_1+E_2}$, $g_1=E_1-\dfrac{E_1E_2}{E_1+E_2}$. Here, g_0 is the so-called long-term modulus of concrete and (g_0+g_1) is the so-called short-term modulus of concrete.

In three-dimensional stress state, we suppose that the viscosity does not have any influence on bulk strain. Similar to Eq.(7), we can obtain the three-dimensional viscoelastic stress-strain relationship as follows

$$\begin{cases}S_{ij}=2G_0e_{ij}(t)+\int_0^t 2G_1\mathrm{e}^{-\alpha(t-\tau)}\dfrac{\mathrm{d}e_{ij}}{\mathrm{d}\tau}\mathrm{d}\tau\\ \sigma_{kk}=3K_0\varepsilon_{kk}(t)+\int_0^t 3K_1\mathrm{e}^{-\mathcal{K}(t-\tau)}\dfrac{\mathrm{d}\varepsilon_{kk}}{\mathrm{d}\tau}\mathrm{d}\tau\end{cases} \tag{8}$$

where $G_0=\dfrac{g_0+g_1}{2(1+\nu_0)}$, $G_1=\dfrac{g_0}{2(1+\nu_1)}$, $K_0=\dfrac{g_0+g_1}{3(1-2\nu_0)}$, $K_1=\dfrac{g_0}{3(1-2\nu_1)}$, and $\mathcal{K}$=0.

The stress-strain relationship of concrete will be related to the loading history if creep is considered. When we deal with such nonlinear problems by the finite-element method, the Newton's method is always adopted and the incremental constitutive relationship should be obtained accordingly.

If the variable t in Eq.(8) is discretized, the following equation can be obtained

$$\begin{cases}S_{ij,m+1}=2G_0\cdot e_{ij,m+1}+2G_1\cdot H_{ij,m+1}\\ \sigma_{kk,m+1}=3K_0\cdot\varepsilon_{kk,m+1}\end{cases} \tag{9}$$

where $H_{ij,m+1}=\int_0^{t_{m+1}}\mathrm{e}^{-\alpha(t_{m+1}-\tau)}\dfrac{\mathrm{d}e_{ij}}{\mathrm{d}\tau}\mathrm{d}\tau$. Supposing that the following equation holds in the time slice $[t_m,t_{m+1}]$

$$\frac{\mathrm{d}e_{ij}}{\mathrm{d}\tau}\approx\frac{e_{ij,m+1}-e_{ij,m}}{t_{m+1}-t_m}=\frac{\Delta e_{ij,m}}{\Delta t_m} \tag{10}$$

Therefore the following expression can be deduced

$$\begin{aligned}H_{ij,m+1}&=\int_0^{t_m}\mathrm{e}^{-\alpha(t_{m+1}-\tau)}\frac{\mathrm{d}e_{ij}}{\mathrm{d}\tau}\mathrm{d}\tau+\int_{t_m}^{t_{m+1}}\mathrm{e}^{-\alpha(t_{m+1}-\tau)}\frac{\mathrm{d}e_{ij}}{\mathrm{d}\tau}\mathrm{d}\tau\\&=H_{ij,m}\cdot\mathrm{e}^{-\alpha\Delta t_m}+\frac{1-\mathrm{e}^{-\alpha\Delta t_m}}{\alpha\Delta t_m}\Delta e_{ij,m}\end{aligned} \tag{11}$$

Introduction of Eq.(15) into Eq.(13) yields the following incremental relations

$$\begin{cases}\Delta S_{ij,m}=S_{ij,m+1}-S_{ij,m}=2\left(G_0+G_1\cdot\dfrac{1-\mathrm{e}^{-\alpha\Delta t_m}}{\alpha\Delta t_m}\right)\Delta e_{ij,m}\\ \qquad\qquad+2G_1(\mathrm{e}^{-\alpha\Delta t_m}-1)H_{ij,m}\\ \Delta\sigma_{kk,m}=3K_0\Delta\varepsilon_{kk,m}\end{cases} \tag{12}$$

From Eq.(12), the three-dimensional incremental viscoelastic constitutive relations of concrete can be easily deduced as follows

$$\Delta\sigma_{ij,m}=\bar{\boldsymbol{D}}_m\Delta\varepsilon_{ij,m} \tag{13}$$

where

$$\bar{\boldsymbol{D}}_m=\begin{bmatrix}A+\frac{4}{3}B & A-\frac{2}{3}B & A-\frac{2}{3}B & 0 & 0 & 0\\ A-\frac{2}{3}B & A+\frac{4}{3}B & A-\frac{2}{3}B & 0 & 0 & 0\\ A-\frac{2}{3}B & A-\frac{2}{3}B & A+\frac{4}{3}B & 0 & 0 & 0\\ 0 & 0 & 0 & B & 0 & 0\\ 0 & 0 & 0 & 0 & B & 0\\ 0 & 0 & 0 & 0 & 0 & B\end{bmatrix},$$

$B=G_1+(G_0-G_1)\dfrac{1-\mathrm{e}^{-\alpha\Delta t_m}}{\alpha\Delta t_m}$, A=K_0, and the time step Δt_m will be sufficiently short.

Equilibrium equation

According to the standard process of the finite-element method, the element stiffness matrix of 3D-VLE can be derived by taking advantage of the virtual work principle. The variable t is discretized for the sequence t_0=0, t_1, t_2, …, t_m, t_{m+1}, …, t_M=T, and the corresponding load vector being, respectively, $\boldsymbol{R}_0$, $\boldsymbol{R}_1$, $\boldsymbol{R}_2$, …, $\boldsymbol{R}_m$, $\boldsymbol{R}_{m+1}$, …, $\boldsymbol{R}_M$. Thus the equilibrium equation at time t_m can be written as follows

$$\begin{aligned}\boldsymbol{\psi} &= \sum\int_{V_e} \boldsymbol{B}^t \boldsymbol{\sigma}_{m+1} \mathrm{d}V - \boldsymbol{R}_{m+1} \\ &= \sum\int_{V_e} \boldsymbol{B}^t (\boldsymbol{\sigma}_m + \Delta\boldsymbol{\sigma}_m) \mathrm{d}V - \boldsymbol{R}_{m+1} \\ &= \bar{\boldsymbol{K}}_m \cdot \Delta\boldsymbol{u}_m - \Delta\bar{\boldsymbol{R}} = 0 \end{aligned} \tag{14}$$

where $\bar{\boldsymbol{K}}_m = \sum\int_{V_e} \boldsymbol{B}^t \bar{\boldsymbol{D}}_m \boldsymbol{B} \mathrm{d}V$, and $\Delta\bar{\boldsymbol{R}}_m = \boldsymbol{R}_{m+1} - \sum\int_{V_e} \boldsymbol{B}^t \boldsymbol{\sigma}_m \mathrm{d}V$. In 3D-VLE, the integral of element stiffness matrix and unbalanced force vector will be dealt with according to different material blocks, as that element is divided into many different material blocks. Therefore the integral form of $\bar{\boldsymbol{K}}_m$ and $\Delta\bar{\boldsymbol{R}}_m$ can be further deduced as follows

$$\begin{aligned}\bar{\boldsymbol{K}}_m &= \sum\int_{V_e} \boldsymbol{B}^{\mathrm{T}} \bar{\boldsymbol{D}}_m \boldsymbol{B} \mathrm{d}V \\ &= \sum_{ie=1}^{ne} \boldsymbol{c}_e^{\mathrm{T}} \cdot \left\{ \sum_{ib=1}^{nb} \int_{-1}^{1}\int_{-1}^{1}\int_{-1}^{1} [\boldsymbol{B}(\xi^{ib}, \eta^{ib}, \zeta^{ib})]^{\mathrm{T}} \cdot [\bar{\boldsymbol{D}}_m^{ib}] \right. \\ &\quad \left. \cdot \left[\boldsymbol{B}(\xi^{ib}, \eta^{ib}, \zeta^{ib}) \right] \cdot |J||J'| \mathrm{d}\xi' \mathrm{d}\eta' \mathrm{d}\zeta \right\} \end{aligned} \tag{23}$$

$$\begin{aligned}\Delta\bar{\boldsymbol{R}}_m &= \boldsymbol{R}_{m+1} - \sum\int_{V_e} B^{\mathrm{T}} \boldsymbol{\sigma}_m \mathrm{d}V \\ &= \sum_{ie=1}^{ne} \boldsymbol{c}_e^{\mathrm{T}} \cdot \left\{ \sum_{ib=1}^{nb} \int_{-1}^{1}\int_{-1}^{1}\int_{-1}^{1} [\boldsymbol{B}(\xi^{ib}, \eta^{ib}, \zeta^{ib})]^{\mathrm{T}} \boldsymbol{\sigma}_m \right. \\ &\quad \left. \cdot |J||J'| \mathrm{d}\xi' \mathrm{d}\eta' \mathrm{d}\zeta' \right\} \end{aligned} \tag{24}$$

where *ne* is the number of elements; *nb* is the number of material blocks in corresponding element; $[\bar{\boldsymbol{D}}_m^{ib}]$ is the three-dimensional increment viscoelastic matrix of the *ib*th material block in corresponding element; $\boldsymbol{c}_e$ is the selection matrix; and $|J'|$ is the value of the Jacobi determinant.

The remaining procedures from the construction of element stiffen matrix to the iteration are the same as those used in the classical time-dependent nonlinear analysis of structures.

Determination of the parameters

To determine the three parameters in the proposed creep model, creep coefficient measurements were carried out on two freely supported prestressed reinforced concrete beams under long-term load (Table 1). The creep coefficients test results are shown in Fig.3. The parameters in the proposed model are fitted by means of the least square method (Table 2). Creep coefficients of the two P.C. beams recommended by CEB-FIP(1978) and ACI(209), for the case that the influence of concrete grade is not considered, are shown in Fig.3. Analytical results obtained by the proposed model, compared to the analytical results obtained by CEB-FIP(1978) and ACI(209), accorded better with experimental results.

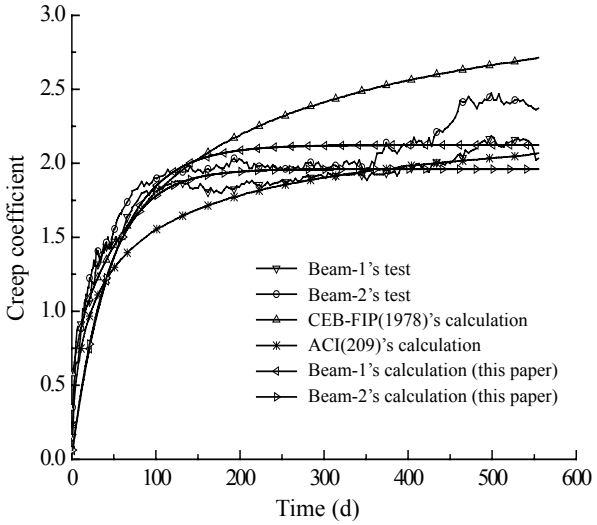

Fig.3 The test and calculating results of creep coefficients

Table 1 Mechanical properties of the two experimental RC beams

Specimen name	Concrete grade	Elastic ratio (GPa)	Poisson's ratio	Load time (d)
Beam-1	C40	32.500	0.1667	555
Beam-2	C45	33.500	0.1667	555

Table 2 Evaluation of three parameters in the proposed creep model

Concrete Grade	Short-term elastic ratio E_1 (GPa)	Long-term elastic ratio $E_1E_2/(E_1+E_2)$ (GPa)	Coefficient E_2/η (GPa·d)
C40	32.50	10.41	772.30
C45	33.50	11.33	735.49

RESULTS AND DISCUSSION

Finite element model of CFT members

By the method of 3D-VLE, the analytical CFT column is divided into 80 elements and 621 nodes. Every element is divided into six material blocks, which include three concrete material blocks, two steel material blocks, and one virtual material block. The finite element model and material blocking of an element are shown in Fig.4. It is necessary to point out that the virtual material block has no effect on the element stiffness matrix, but makes the finite element overall modeling more convenient and avoids dealing with the contact problems arising from the material diversities on the structural cross-section.

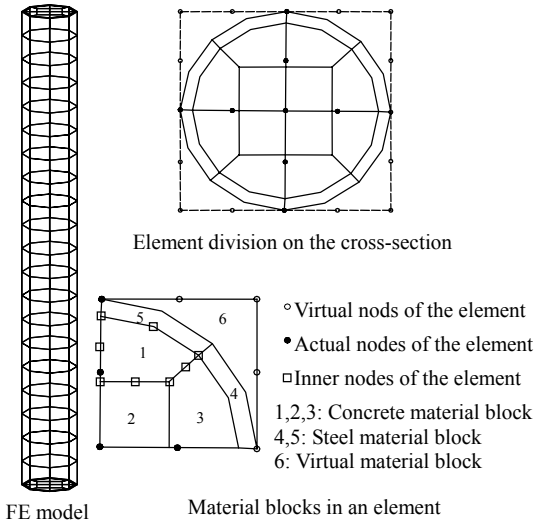

Fig.4 The finite element modeling and material blocks in an element

Test specimens considered in analysis

Experimental investigation on CFT columns under long-term axial and eccentric load were carried out (Tan and Qi, 1987). The mechanical properties of test specimens are presented in Table 3. The complete details of the experiments can be found in the reference (Tan and Qi, 1987).

Comparison of the experimental and calculated results

Here, we introduce two fundamental concepts: (1) Creep strain $\varepsilon_{cc}(t)=\varepsilon(t)-\varepsilon_e$, where $\varepsilon(t)$ is the overall strain at the time of t, and ε_e is the elastic strain in the same loading condition; (2) Creep coefficient $\varphi(t)=\varepsilon_{cc}(t)=\varepsilon(t)/\varepsilon_e$. We assume that the compressive strain is "+" and tensile strain is "–".

Creep strain curves $\varepsilon_{cc}(t)$~t of the four specimens are shown in Fig.5. From the comparison between the analytical and experimental results, we could draw the conclusion as the follows:

1. The proposed method 3D-VLE, is capable of predicting the time-dependent behavior of CFT members under long-term axial and eccentric load to acceptable accuracy.

2. Creep influence on CFT members is very obvious. For example, when the load time is 180 d, the analytical results of creep strain were about from 250×10^{-6} to 400×10^{-6}, and the experimental results were about from 300×10^{-6} to 400×10^{-6}. The evaluated values of creep coefficients were between 0.30 and 0.80 (Table 4). Comparison of analytical and experimental results showed that they agreed well.

3. Creep strain curve $\varepsilon_{cc}(t)$~t begins to be horizontal when the load time is 90 d and creep phenomenon nearly stops when the load time is 120 d. So we think that it is sufficiently accurate to consider the influence of concrete creep on CFT structures when the load time T is about between 120 d and 150 d, since core concrete creep had finished more than 95% by the time.

4. Because the proposed creep model is directly applied to three-dimensional finite element 3D-VLE, unlike previous methods, the method proposed in this paper can take into account the arbitrary loading con-

Table 3 Mechanical properties of the experimental CFT specimens

Member numbering	T (d)	L (mm)	D (mm)	$4\frac{h}{D}$	$\frac{2e}{D}$	$\frac{N}{N_j}$	N_j (kN)	Core concrete		Steel	
								E_c (GPa)	f_{ck} (MPa)	E_s (GPa)	f_y (MPa)
No. I	360	432.0	108.0	0.0770	0.00	0.399	536.0	33.50	33.6	220.0	315.0
No. II	180	450.0	114.0	0.0716	0.40	1.015	271.2	33.50	33.6	197.0	332.0
No. III	180	450.0	114.0	0.0740	0.55	0.638	390.5	33.50	33.6	197.0	332.0
No. IV	180	450.0	114.0	0.0855	0.80	0.673	280.0	33.50	33.6	197.0	332.0

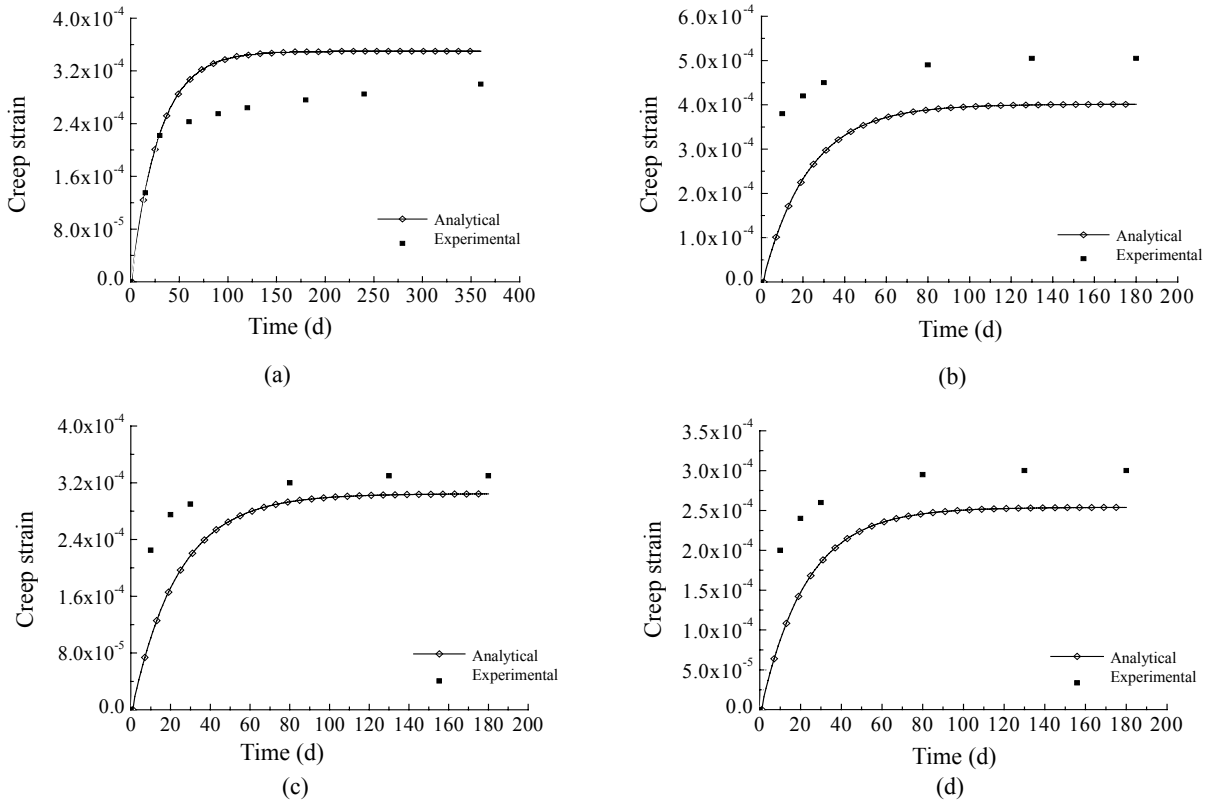

Fig.5 Creep curve $\varepsilon_{cc}(t)$~t of specimen No. I (a); No. II (b); No. III (c); No. IV (d)

Table 4 Calculating results of creep strains and creep coefficients

Member numbering	Elastic strain ε_e ($\times10^{-6}$)	Creep strain $\varepsilon_{cc}(t)$ ($\times10^{-6}$)		Creep coefficient $\varphi(t)$
		Analytical results	Experimental results	
No. I	462.5	350.0	300	0.757
No. II	1039.6	401.2	505	0.386
No. III	692.8	304.3	330	0.439
No. IV	657.0	253.9	300	0.386

dition and geometrical form, while the required precision for engineering can be easily achieved. Furthermore, the application of virtual nodes and virtual material blocks in the FE modeling has many merits, for example, the number of required elements can be greatly decreased and computational efficiency can be greatly improved. Therefore the method proposed in this paper can be extensively applied in engineering practice, especially in complicated composite structures.

INFLUENCING FACTORS OF CREEP

As experimental and theoretical investigations on time-dependent behaviours of CFT structures had seldom been reported in the past study, this paper took CFT members with representative geometry and sectional dimensions as examples for studying the influencing regularities of many factors, which included the ratio of long-term load to strength $n=N_L/N_u$, the slenderness ratio $\lambda=4L/D$, the steel ratio $\omega=4h/D$, and the eccentricity ratio $\theta=2e/D$, on core concrete creep. These research findings can be consulted in engineering practice.

Ratio of long-term load to strength n

The mechanical properties of the four specimens included in the calculation can be detailed as follows: sectional dimensions were $D\times h=120\times4$ (mm^2). The

age of the concrete at loading was 28 d. Core concrete was C45 and steel tube was Q345. The slenderness ratio λ was 60 and the eccentricity ratio θ was 0.0. The ratio of long-term load to strength n was, 0.4, 0.6, 0.8, and 1.0, respectively. The strengths N_u of the analytical specimens were all supposed to be 1.0 kN. We neglected material plasticity in the numerical calculation. The influencing regularity of n on creep coefficient $\varphi(t)$ of CFT structures is presented in Fig.6a.

As shown in Fig.6a, creep coefficient curves $\varphi(t)$~t are basically the same with the variance of n. When load time was t=300 d, creep coefficients $\varphi(t$=300 d) of the four calculating specimens were all about 0.60. But creep strain had linear relations with the factor n.

Slenderness ratio λ

The mechanical properties of the four specimens included in the calculation can be detailed as follows sectional dimensions were $D\times h$=120×4 (mm^2). The age of the concrete at loading was 28 d. Core concrete was C45 and steel tube was Q345. The eccentricity ratio θ was 0.0. The long-term load N_L was supposed to be 1.0 kN. The slenderness ratio λ was, 40, 60, 80, and 100, respectively. The influencing regularity of λ on creep coefficient $\varphi(t)$ of CFT structures is presented in Fig.6b.

As shown in Fig.6b, creep coefficient curves $\varphi(t)$~t of the four specimens are all basically accorded with the variance of λ. When load time was t=300 d, creep coefficients were all about 0.60. Such phenomenon also confirmed our supposition that concrete creep arises mainly from shear viscosity and that the influence of bulk viscosity is very little.

Steel ratio ω

The mechanical properties of the four specimens included in the calculation can be detailed as follows: sectional dimension was D=120 mm. The age of the

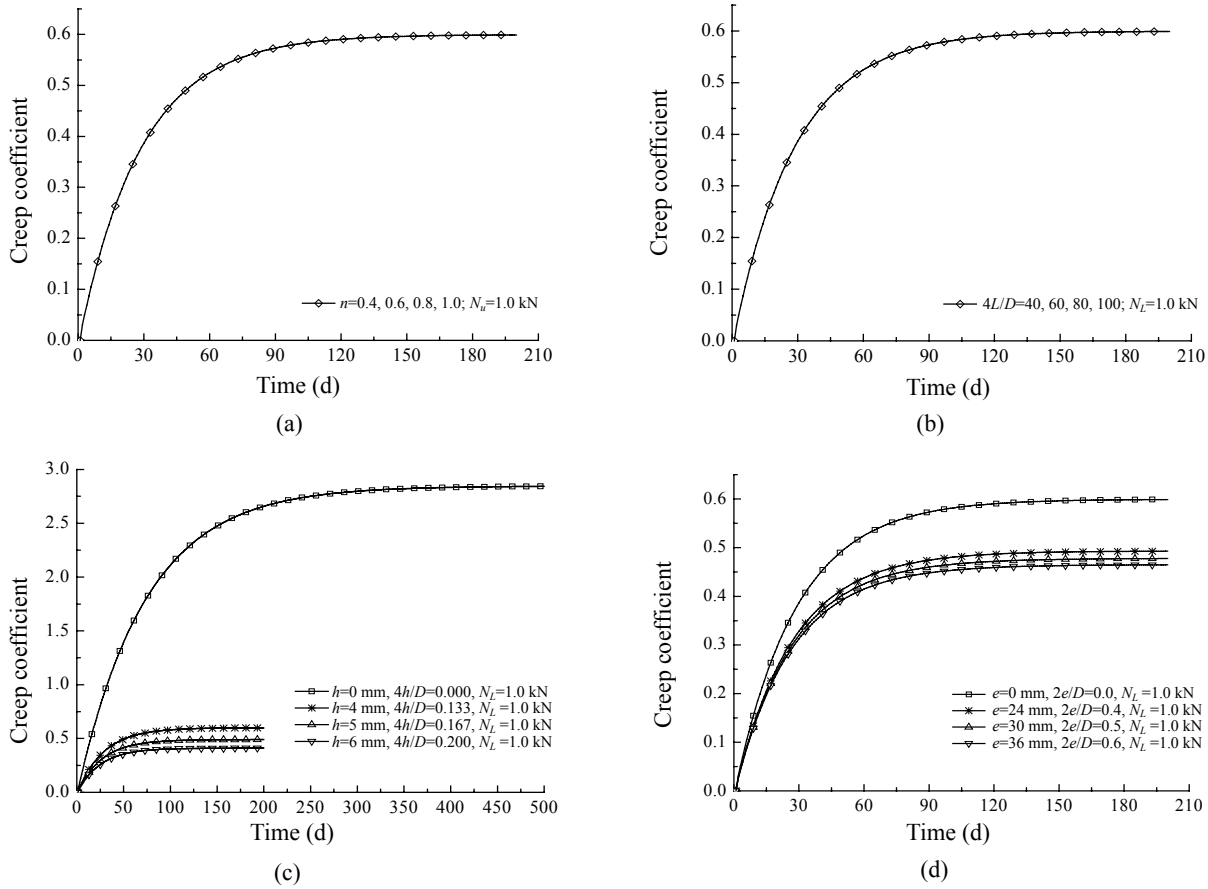

Fig.6 Curve $\varphi(t)$~t (a) when θ=0.0, 0.4, 0.5, 0.6; (b) when λ=40, 60, 80, 100; (c) when ω=0.0, 0.133, 0.167, 0.2; (d) when θ=0.0, 0.4, 0.5, 0.6

concrete at loading was 28 d. Core concrete was C45, and steel tube was Q345. The eccentricity ratio θ was 0.0. The long-term load N_L was supposed to be 1.0 kN. The slenderness ratio λ was 60. The wall thickness h of steel tube was 0 mm, 4 mm, 5 mm, and 6 mm, respectively, that is to say the steel ratio ω was about, respectively, 0.00, 0.133, 0.167, and 0.200. The influencing regularity of ω on creep coefficient $\varphi(t)$ of CFT structures is presented in Fig.6c.

It was not difficult to find that the creep coefficient curve $\varphi(t)$~t of the plain concrete column (ω=0.0) did not begin to be horizontal until load time was 360 d, but that of CFT columns (ω=0.133, 0.167, and 0.200) started to be horizontal when load time was 120 d. When load time was t=300 d, creep coefficients $\varphi(t$=300 d) of the four analytical specimens were, respectively, 2.798, 0.600, 0.490, and 0.411. But when load time was t=500 d, creep coefficient $\varphi(t$=500 d) of the plain concrete columns was about 2.843. From the above research results, it is not difficult to find that the influence of creep on plain concrete column was obviously greater than that on CFT columns. On the other side, they show that the interaction of steel tube and core concrete greatly improved the mechanical properties of the core concrete under long-term loading.

Eccentricity ratio θ

The mechanical properties of the four specimens included in the calculation can be detailed as follows: sectional dimensions were $D\times h$=120×4 (mm^2). The age of the concrete at loading was 28 d. Core concrete was C45 and steel tube was Q345. The long-term load N_L was supposed to be 1.0 kN, and the slenderness ratio λ was 60. The eccentricity ratio θ was, respectively, 0.0, 0.4, 0.5, and 0.6. The influencing regularity of θ on creep coefficient $\varphi(t)$ of CFT structures is presented in Fig.6d.

As shown in Fig.6d, the eccentricity ratio θ had relatively great influence on the creep of the CFT columns. With the increase of the eccentricity ratio θ, the creep strain $\varepsilon_{cc}(t)$ of the maximum compression-side on the midspan cross-section increases accordingly, but creep coefficient $\varphi(t)$ gradually decreases. For example, when load time t was 300 d and long-term load N_L was 1.0 kN, creep strains $\varepsilon_{cc}(t$=300 d) of the four analytical specimens were, respectively, 0.94×10^{-6}, 1.23×10^{-6}, 1.30×10^{-6}, and 1.38×10^{-6}. However, creep coefficients $\varphi(t$=300 d) were, respectively, 0.600, 0.493, 0.478, and 0.465. In short, with the increase of θ, creep strain $\varepsilon_{cc}(t)$ linearly increases, whereas creep coefficient $\varphi(t)$ linearly decreases.

CONCLUSION

The main conclusions from the investigations presented in this paper are summarized as follows:

1. The method of three-dimensional virtual laminated element (3D-VLE) was developed to investigate the mechanical properties of concrete filled steel tube (CFT) structures. A three-parameters viscoelastic model, which represents the combined effect of the Maxwell and Voigt models, is adopted as an approach to investigate the time-dependent behaviour of CFT columns. The proposed finite element method can consider the diversities of materials on the structural cross-section. As virtual nodes and material blocks probable exist in the element, thus on one hand, every element can be divided into many material blocks and different blocks can be composed of different materials, even empty materials. The number of needed elements can be greatly decreased and computational efficiency is greatly improved. Therefore the proposed finite element method will have wide applications for composite structures, such as CFT.

2. After evaluation of the three parameters in the proposed creep model, the creep phenomenon of CFT columns subject to long-term axial and eccentric load can be investigated. Comparison between the time-dependent behaviour displayed by the experimental test results (Tan and Qi, 1987), and those obtained by the proposed method showed good agreement between them.

3. In view of the fact that experimental and theoretical investigations on time-dependent behaviours of long CFT columns were seldom reported in past study, this paper takes CFT columns with representative geometry and sectional dimensions as examples and adopts the proposed method as an approach to investigate the influencing regularities of many factors, which include the ratio of long-term load to strength n, the slenderness ratio λ, the steel

ratio ω, and the eccentricity ratio θ, on the core concrete creep. Those research findings can be consulted in the engineering practice and design.

References

ACI Committee 209, 1992. Prediction of Creep, Shrinkage and Temperature Effects in Concrete Structures. ACI 209 R-92, ACI, SP-70.

Bažant, Z.P., 2001. Prediction of concrete creep and shrinkage: past, present and future. *Nuclear Engineering and Design*, **203**(1):27-38.

Bažant, Z.P., Panula, L., 1980. Creep and shrinkage characterization for analyzing prestressed concrete structures. *PCI Journal*, **25**(3):86-112.

CEIB (Comité Euro-International du Béton), 1993. CEB-FIP Model Code 1990 for Concrete Structures. Bulletind'information No. 213/214, Lausanne.

Cheng, X., Ye, G., Wang, J., 2004a. Theoretical investigation of creep in concrete filled steel tube columns under long-term load. *Journal of Zhejiang University* (*Engineering Science*), **38**(8):68-77 (in Chinese).

Cheng, X., Ye, G., Xu, X., 2004b. FEM analysis of buckling bearing capacities of concrete filled steel tube columns under eccentric load. *Journal of Zhejiang University* (*Engineering Science*), **38**(1):79-85 (in Chinese).

Ichinose, L.H., Watanabe, E., Nakai, H., 2001. An experimental study on creep of concrete filled steel pipes. *Journal of Constructional Steel Research*, (57):453-466.

Nakai, H., Kurita, A., Ichinose, L.H., 1991. An Experimental Study on Creep of Concrete Filled Steel Pipes. Proceedings of 3rd International Conference on Steel-Concrete Composite Structures, Fukuoka, Japan, p.55-60.

Qi, J., 1986. Experimental Investigation of the Effects on the Strength of Concrete Filled Tubular under Eccentric Load. Harbin Architectural and Civil Engineering Institute.

Tan, S., Qi, J., 1987. Experimental investigation of the effects on the strength of concrete filled tubular compression members load. *Journal of Harbin Architectural and Civil Engineering Institute*, (2):10-24.

Terrey, P.J., Bradford, M.A., Gilbert, R.I., 1994. Creep and Shrinkage of Concrete in Concrete-filled Circular Steel Tubes. Proc. of 6th Inter. Symposium on Tubular Structures, Melbourne, Australia, p.293-298.

Xu, X., Cai, R., 1993. A new plat shell element of 16 nodes 40 degnees of freedom by relatiue displacement method. *Communications in Numerical Methods in Engineering*, (9):15-20.

Xu, X., Cheng, X., Ling, D., 2002. Finite element analysis of load bearing capacities of concrete filled steel tube columns under axial load. *ACTA Mechanical Solid Sinica*, **23**(4):419-425.